PHYSICAL REVIEW
LETTERS

VOLUME 32 4 MARCH 1974 NUMBER 9

# Breit Interaction and Double $K$ Vacancies in Nuclear Transitions

J. P. Desclaux
*Centre d'Etudes de Limeil, 94190 Villeneuve St. Georges, France*

and

Ch. Briançon, J. P. Thibaud, and R. J. Walen
*Centre de Spectrométrie Nucléaire et de Spectrométrie de Masse, 91406 Orsay, France*
(Received 17 December 1973)

It is shown that the energy shift of $K$ x rays emitted by an atom doubly ionized in the $K$ shell comprises a 16% Breit-interaction contribution for $Z=81$ and thus constitutes a sensitive test of these corrections. The calculated shift of the $K\alpha_1$ line agrees with the present experiment (1160 ±70 eV). This invalidates the much larger 2100-eV shift, reported by another group, which appears to be due to spurious effects.

Electrostatic terms are highly predominant in electronic binding-energy calculations. Additional corrections (magnetic interaction, self-energy, vacuum polarization, and retardation) are highly $Z$ dependent. For low and medium $Z$ they are small if not negligible and, for $Z=100$, their contribution to the binding energy amounts to 0.7%.[1,2] For super-heavy and transient ultrahigh $Z$ atoms, these terms would become increasingly important and a more sensitive test than the comparison with experimental binding energies appears necessary.

An experimental quantity quite sensitive to Breit terms is the difference of atomic inner-shell binding energies in neutral and deep-shell-ionized atoms: A partial compensation of electrostatic terms raises the energy correcting terms to 16% of the total shift.

In the following we restrict ourselves to $K$ and $L$ shells, with particular emphasis on the $K$ binding energy in the presence or not of a $K$ spectator vacancy. If we define $B_{\lambda'}{}^{(\lambda)}$ as the binding energy of a $\lambda'$ electron in presence of a configuration, described by $(\lambda)$, involving a vacancy, the shift with respect to the neutral-atom binding energy $B_{\lambda'}$ is denoted

$$\Delta B_{\lambda'}{}^{(\lambda)} = B_{\lambda'}{}^{(\lambda)} - B_{\lambda'}. \tag{1}$$

The resulting shift for x rays is then given by a difference of two quantities $\Delta B$,

$$S(\lambda; \lambda'' \to \lambda') = \Delta B_{\lambda'}{}^{(\lambda)} - \Delta B_{\lambda''}{}^{(\lambda)} \tag{2}$$

which leads, for example, in the case of a $K\alpha_1$ line and an initially empty $K$ shell, to

$$S(1s; 2p \to 1s) = \Delta B_{1s}{}^{(1s^1 2p^4)} - \Delta B_{2p}{}^{(1s^1 2p^4)}, \tag{3}$$

where $p$ stands for the $p_{3/2}$ subshell and where $(\lambda)$ refers to the occupation of the involved shells only (for sake of brevity only the spectator vacancy is specified in the $S$-shift expression).

Double vacancies in the $K$ shell occur, with low probability, in nuclear processes like electron capture and internal conversion.

The only measurements for high $Z$ have been given by Briand *et al.*[3] and concern the disintegration

$$^{203}\mathrm{Hg} \xrightarrow{\beta^-} {}^{203}\mathrm{Tl}^* \xrightarrow{279\ \mathrm{keV}} {}^{203}\mathrm{Tl}.$$

These authors have found experimental energy shifts for $K\alpha_1$ and $K\alpha_{1,3}$ lines of 2130 and ~2500 eV, respectively, with a total double-$K$ ionization probability equal to $2.5\times10^{-4}$ per $K$ conversion of 279-keV transition.

A puzzling theoretical situation arose with the strong disagreement we found between these values and our calculated energy shifts, which led us to investigate thoroughly the $Kx$-$Kx$ coincidence spectrum in the $^{203}$Hg decay.

Two planar (5 cm$^2$) Ge-Li detectors (0.8 keV at 100 keV) were used in a large-angle close geometry. Special care was devoted to avoid spurious coincidences arising from extraneous materials and back scattering since the events searched for have very low probability. The source (diam =0.3 mm) was set in the center of a tantalum diaphragm (with a 1-mm opening) so as to minimize scattering from one detector into the other one. Electrons were absorbed by copper oxide. The purity of these absorbers is essential to avoid any trace of lead whose fluorescence spectrum would yield perturbing x-ray lines lying 2100 and 2360 eV above the $K\alpha_1$ and $K\beta_{1,3}$ lines of thallium, respectively.

Three separate runs, 11 days long on the average, were carried out with a low counting rate (1000 counts/sec) in order to maintain random coincidences at a convenient level. Overall stability of electronics was $\sim10^{-4}$ during each run, limiting the measured peak drifts to 10 eV.

Figure 1 shows schematically the peaks one observes in a three-dimensional display. The peaks are represented by their contour at $\frac{1}{10}$ of their height. The main peaks (full circles) contain coincidences between the $K$ x rays of the $K$-converted 279-keV transition and either the x rays of the internal ionization accompanying $\beta$ decay feeding this level, or the bremsstrahlung (internal and external). These peaks are not shifted since the half-life of the nuclear excited state is long enough to ensure neutralization of the atom before the $K$-conversion vacancy is created.

The dashed circles represent the coincidences we are looking for: The different combinations of $K\alpha_1$ and $K\alpha_2$ coincidences are given in detail. The most important energy shifts ($a$ and $b$) pertain to the first $x$ emission in presence of a $K$ spectator vacancy, the less important shifts ($c$, $d$, $e$, and $f$) to the second emission with an $L$ spectator vacancy. The analysis neglects the intermediate-coupling-scheme splittings which cannot be detected with the present energy resolution. Those $\Delta B$'s which contain splittable terms are therefore mean values.

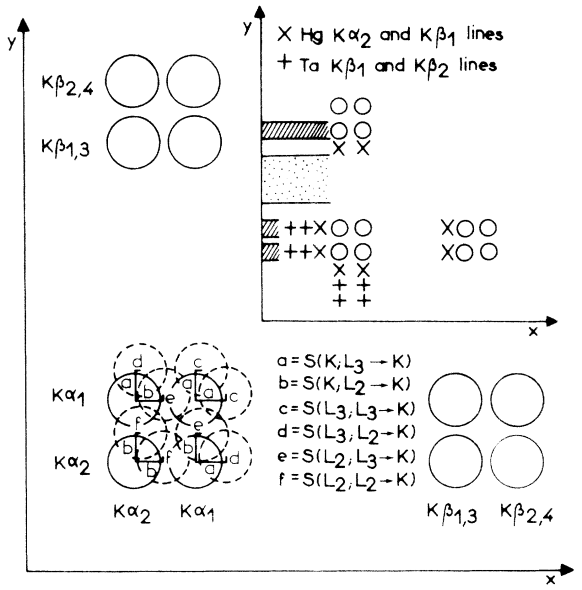


FIG. 1. Schematic biparametric representation of the $x$-$x$ coincidences. Full circles, main unshifted peaks; dashed circles, the various satellite peaks of the $K\alpha$-$K\alpha$ zone. The energy shift of each satellite comprises two components. The $a$ and $c$ shifts pertaining to the $K\alpha_1$-$K\alpha_1$ coincidences are given in Table I. X rays of Hg and Ta arise from the diaphragm and from mercury in the source. The way of summing over $y$ channels, as explained in the text, is shown in the inset.

Figure 2 reproduces the experimental spectra of one of the runs with a summation over the $y$ channels as shown on the inset of Fig. 1: The hachured zones yield the curve 1 containing the shifted peaks. Besides the strongly shifted first-emitted x ray, many components add up together, resulting from the $y$ summation over $K\alpha$ and $K\beta$ peaks, and are related to the second-emitted x ray, in the presence of an $L$ or $M$ spectator vacancy, with eventual splitting of the initial and final states. These contributions, however, have small energy shifts and low intensities as compared to the main line and have a negligible influence on the analysis shown on the inset of Fig. 2.

The dotted zones correspond to a sum of processes (coincidences with various bremsstrahlungen) for which no energy shift occurs. This curve 2, normalized on the $K\alpha_1$ line of curve 1, supplies the profile of the normal $K\alpha_1$ line with which the complex $K\alpha_1$ line of curve 1, after subtraction of the background, is analyzed by means of a nonlinear least-squares-fit code.

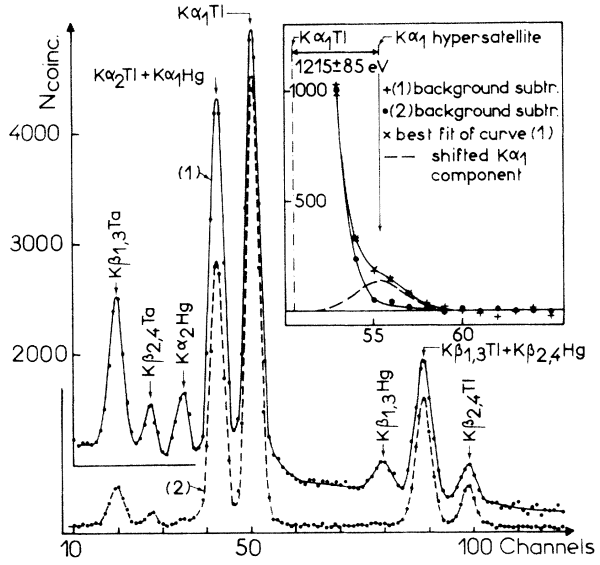


FIG. 2. Typical experimental coincidence spectra. Curve 1 is obtained by summing, along the $y$ axis, over the main Tl x-ray peaks as shown on Fig. 1 (hachured zone). Curve 2 corresponds to the dotted zone and provides the line profile used for the decomposition shown on the inset. In the nonshifted $K\alpha_1$ Tl line, random coincidences amount to less than 5%.

Absolute intensities have been deduced from measurements with calibrated standard sources and from the time-to-amplitude converter efficiency. The energy shifts obtained from the three runs are $1080 \pm 170$, $1075 \pm 130$, and $1215 \pm 85$ eV. The weighted average yields $1160 \pm 70$ eV for the $K\alpha_1$ shift, $T_{KK}/T_K = (4.0 \pm 1.5) \times 10^{-5}$. This experimental intensity is obtained assuming the same fluorescence yield $\omega_K$ and the same relative $K\alpha_2$, $K\alpha_1$, $K\beta$ x-ray intensities for both $K$-shell vacancies.

At the position where one should find the hypersatellite mentioned by Briand *et al.*,[3] no line is observed with an upper limit of $\sim 10^{-5}$ per $K$ conversion. The shifted lines observed by these authors are to be attributed to fluorescence x rays of lead impurities, which occur at the same energies.

The shift defined by relations (1) and (2) can also be expressed in terms of the total energies:

$$S(1s; 2p \rightarrow 1s) = E(1s^1 2p^3) - E(1s^0 2p^4) + E(1s^1 2p^4) - E(1s^2 2p^3). \quad (4)$$

The total energies have been calculated with a relativistic Dirac-Fock code written by one of us (J.P.D.). In order to determine the radial wave functions, the total Hamiltonian is reduced to a sum of Dirac one-electron Hamiltonians plus the classical Coulomb repulsion terms. After self-consistency has been obtained, the Breit operator is introduced as a first-order perturbation to take partially into account the relativistic electron-electron interaction. Higher-order relativistic corrections, which contribute to the Lamb shift, have been neglected. Since the contributions to the Lamb shift (self-energy and vacuum polarization) involve one-body operators, it is easily seen from Eq. (4) that the contributions to $S(\lambda; \lambda'' \rightarrow \lambda')$ due to these operators cancel out in the frozen-orbital approximation and arise only because of the rearrangement of each configuration involved. Furthermore, the Lamb-shift contribution is almost negligible for the $2p$ electron binding energy (Ref. 2) and only the rearrangement of the $K$ shell will give a small contribution to higher-order relativistic corrections. As the influence of correlation effects has not been introduced, it would be meaningless to consider these small corrections due to the Lamb shift.

TABLE I. Total energies for thallium (in eV), where column I is the unperturbed Dirac-Fock energy, column II has the magnetic interaction included, and column III has the full Breit interaction included.

| | I | II | III |
|---|---|---|---|
| $1s^2 2p^4$ [a] | −551 678 | −550 957 | −551 035 |
| $1s^2 2p^3$ | −538 980 | −538 302 | −538 373 |
| $1s^1 2p^4$ [a] | −465 678 | −465 299 | −465 354 |
| $1s^2 2p^2$ | −526 025 | −525 389 | −525 451 |
| $1s^1 2p^3$ | −452 608 | −452 265 | −452 315 |
| $1s^0 2p^4$ | −378 272 | −378 032 | −378 062 |
| $S(2p; 2p \rightarrow 1s)$ | 115 | 121 | 117 |
| $S(1s; 2p \rightarrow 1s)$ [b] | 1034 | 1230 | 1234 |

[a]The calculated $K$ binding energy including 161 eV for the Lamb shift (Ref. 4) is 85 520 (experimental value: 85 530).

[b]Experimental value: $1160 \pm 70$.

The influence of the splittings is less obvious. The calculated splittings of the $KL_3$ ($^3P_2 - {}^3P_1$) and $L_3L_3$ ($^3P_2 - {}^3P_0$) hole configurations are 40 and 66 eV, respectively. A difference between the experimental value and the calculated one (weighting factors $2J+1$) will arise from the intensity ratios which are not actually known. This difference should not exceed 15 eV for the $S(K; L_3 \rightarrow K)$ shift.

Although it is difficult to estimate the overall

uncertainty of the theoretical value, we may nevertheless expect an error smaller than 35 eV. The main contributions to this uncertainty should arise from neglected splitting (15 eV) and correlation (20 eV) effects. This latter estimate is supported by the calculated $K$-electron binding energies[4] which agree with experimental results within 10 eV, even if one neglects correlation effects.

In Table I we list total average energies calculated with or without the above mentioned Breit corrections (magnetic and retardation) and without the Lamb shift.

Comparison between the various values of the shifts shows that the magnetic interaction correction (which amounts to about 16%) is essential to obtain a good agreement with the experimental result.

[1]M. S. Freedman, F. T. Porter, and J. B. Mann, Phys. Rev. Lett. 28, 711 (1972).

[2]B. Fricke, J. P. Desclaux, and J. T. Waber, Phys. Rev. Lett. 28, 714 (1972).

[3]J. P. Briand, M. Frilley, P. Chevallier, A. Johnson, J. P. Rozet, M. Tavernier, and A. Touati, in *Proceedings of the International Conference on Inner-Shell Ionization Phenomena and Future Applications, Atlanta, Georgia, 1972,* edited by R. W. Fink, S. T. Manson, J. M. Palms, and P. V. Rao, CONF-720404 (U. S. Atomic Energy Commission, Oak Ridge, Tenn., 1973), pp. 1930, 1940.

[4]A. M. Desiderio and W. R. Johnson, Phys. Rev. A 3, 1267 (1971).

# Stimulated Raman and Brillouin Scattering: Parametric-Instability Explanation of Anomalies*

M. Sparks
*Xonics, Incorporated, Van Nuys, California 91406*
(Received 7 November 1973)

The Raman and Brillouin processes have important sharp-threshold parametric instabilities that afford explanations of long-standing anomalies in stimulated-scattering and self-focusing experiments. Below the threshold intensity $I_c$, the gain is nonexponential and greater than that of previous theories of stimulated scattering, and at the threshold the Stokes intensity increases nearly discontinuously. Typically, $I_c \sim 10^9$ W/cm$^2$ for a number of gases, liquids, and solids. The theoretical results agree well with previous experimental results.

Some of the major problems of the physics of quantum electronics, which concern stimulated scattering, have remained unsolved in spite of numerous investigations. These include "oscillations" observed in a number of systems with insufficient gain to cause oscillations, insensitivity of the "oscillation" threshold to changes in gain, deviations from exponential gain, sharpness of changes in Stokes output, anomalously high gain in a number of systems, a theoretical gain that is orders of magnitude too small to explain the complete conversion to Stokes radiation in the self-focused forward-moving focal region observed in several liquids, and continued difficulty in explaining the limiting diameter of self-focused beams.

These anomalies are explained in terms of a parametric instability that has been overlooked previously even though parametric instabilities were well known in ferromagnetic resonance, plasma physics, and radio-wave propagation.[1,2] In ferromagnetic systems, instabilities are observed in samples that are small with respect to the microwave-photon wavelength. The stimulated scattering processes are more complicated since propagation of the photons must be considered.

By using the well-known perturbation theory result for the rate of transitions between states, the rate of creation of Stokes photons per volume $V$ by the Raman process can be written down immediately as $C[(n_S + n_Q + V^{-1})n_L - n_S n_Q]$, where $C = 2\pi |V_R/\hbar|^2 V \delta(\tilde{\omega})$, with $V_R$ the Raman matrix element, the argument of the $\delta$ function $\tilde{\omega} \equiv \omega_L - \omega_S - \omega_Q$, and the subscripts $L$, S, and $Q$ denote laser, Stokes, and phonon. The $n$'s are boson occupation numbers, which come from the well-known three-boson factor $n_L(n_S + V^{-1})(n_Q + V^{-1}) - (n_L + V^{-1})n_S n_Q$.[1] In gases and liquids, "phonon" means the nearly dispersionless excitation of the system that is excited in the Raman process.